NOTES AND CORRESPONDENCE

The Generation of Mesospheric Planetary Waves by Zonally Asymmetric Gravity Wave Breaking[1]

JAMES R. HOLTON

Department of Atmospheric Sciences, University of Washington, Seattle WA 98195

2 June 1984 and 17 September 1984

ABSTRACT

A semi-spectral numerical model is used to study the influence of a longitudinally varying gravity wave source on the general circulation of the winter mesosphere. The gravity wave source consists of stationary (topographic) waves with a longitudinally varying amplitude distribution that is approximated by the first two terms in a zonal harmonic expansion (i.e., the zonal mean plus planetary wavenumber 1). The computed zonal mean circulation in the mesosphere is nearly the same as that computed for a zonally symmetric gravity wave source of equal amplitude. However, the asymmetric source excites a strong stationary wavenumber 1 disturbance near the level of gravity wave breaking ($\approx$71 km). This disturbance has a zonal wind maximum about ¼ cycle upstream from the gravity wave drag maximum. It is concluded that vertically propagating gravity waves produced in the troposphere are a possible source for mesospheric planetary waves.

1. Introduction

Lindzen (1981) proposed a simple scheme for parameterizing the drag and diffusion generated by breaking internal gravity waves in the mesosphere. His work, together with recent developments in observational techniques based on active remote sensing, has stimulated considerable interest in the generation, propagation and mean flow interaction of internal gravity waves. The subject was reviewed briefly by Lindzen (1984) and more extensively by Fritts (1984). The reader should consult their papers for background and references to the recent literature.

Holton (1983) applied the Lindzen (1981) parameterization in a simulation of the solstice mean global circulation of the mesosphere using a semi-spectral numerical model. He showed that gravity wave drag and diffusion, represented by Lindzen's parameterization, could account for the observed large departure from radiative equilibrium conditions in the mesosphere. In his study the longitudinal dependence was severely truncated to include only the zonal mean and a single zonal wavenumber 1 disturbance. The wave-breaking drag force was assumed, however, to be zonally symmetric so that gravity wave breaking influenced the simulated planetary waves only through induced vertical diffusion (with the diffusion coefficient itself assumed to be zonally symmetric). In reality, gravity wave propagation depends on the three-dimensional distribution of the background flow field. Dunkerton and Butchart (1984) showed that for waves of horizontal scale less than several hundred kilometers, ray paths do not deviate very far in the zonal or meridional direction during the course of their upward propagation from the troposphere to the mesosphere, at least for normal winter wind conditions. Thus, it is reasonable to assume that such waves "see" the local background wind distribution rather than the mean zonal wind. Hence the Lindzen parameterization should, in the presence of a zonally varying background flow, be applied locally. The resulting wave breaking altitude, drag force and diffusion coefficient would all then be longitudinally dependent.

That such longitudinal dependence can be substantial was demonstrated by Schoeberl and Strobel (1984). They examined the longitudinal dependence of wave drag and heat transport in a model with an externally specified longitudinally varying background zonal wind. They found that the altitude of wave breaking and the intensity of the drag and the diffusion of heat and momentum depended sensitively on the local wind profile. For their model parameters (which included a very strongly wavenumber dependent radiative damping) waves were unable to propagate into the mesosphere in regions where the doppler shifted phase speeds were much less than 20 m s^{-1}. Thus, the longitudinally dependent stratospheric winds caused a selective transmission of gravity waves passing through the stratosphere. It seems likely that the resulting longitudinally varying wave drag and diffusion might generate planetary waves in the mesosphere as suggested by Schoeberl and Strobel.

Similarly, zonally asymmetric gravity wave sources may generate planetary waves in the mesosphere due

---

[1] Contribution No. 715, Department of Atmospheric Sciences, University of Washington.

to their zonally asymmetric drag and diffusion even in the absence of planetary waves in the stratosphere. The purpose of this note is to present a preliminary analysis of the structure of a mesospheric planetary wave excited by zonally asymmetric topographic gravity waves propagating through a zonally symmetric stratospheric wind field.

2. The model

The numerical calculations were carried out with the semi-spectral model developed by Holton and Wehrbein (1980) as modified and updated by Holton (1983). For details the reader should refer to those papers. In the experiments reported here the orographic (i.e., stationary) gravity wave source distribution is assumed to be uniform in latitude but to have a longitudinal distribution given by

$$W(\lambda, \phi) = \begin{cases} W_0, & 0 < \lambda - \lambda_0 < \pi \\ 0, & \pi \leq \lambda - \lambda_0 \leq 2\pi, \end{cases}$$

where W_0 is a constant and $\lambda_0 = \pi/4$. Because the numerical model represents the large scale variables in terms of a truncated zonal harmonic expansion, an inverse Fourier transform must be carried out at each time step in order to compute the "local physics" involved in the wave drag parameterization, followed by a Fourier transform to compute the projection of the wave drag and diffusion on the zonal mean and planetary wavenumber 1 modes. This process is analogous to the treatment of parameterized convection in spectral general circulation models.

In the results reported here we have computed the wave breaking level, wave drag forces and vertical momentum diffusion locally at longitudes $\lambda = 0, \pi/2, \pi, 3\pi/2$. These four longitudes are sufficient to determine unaliased projections on the first two terms of a zonal harmonic expansion. The wave source amplitude was adjusted so that the zonal mean wavedrag was nearly equal to that of the zonally symmetric wave source used by Holton (1983).

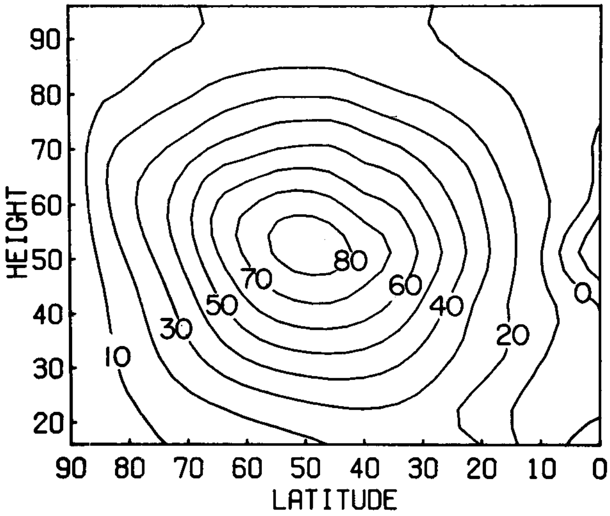

FIG. 1. Latitude–height section of zonal mean wind (m s^{-1}) at winter solstice (day 60).

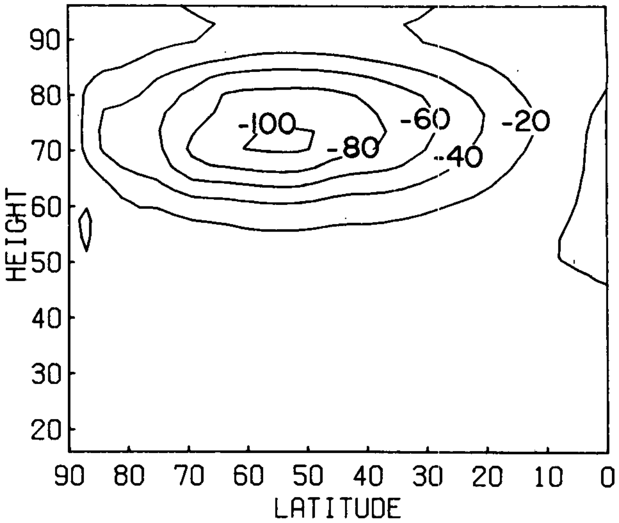

FIG. 2. Zonal mean component of wave drag force (m s^{-1} day^{-1}) at winter solstice (day 60).

With the exception of the zonal dependence specified for the topographic waves, the model parameters were identical to those used in Holton (1983). Thus, in addition to the topographic gravity waves, waves of phase speeds ± 20 m s^{-1} were included to provide the wave drag and diffusion necessary to maintain the mesospheric momentum balance in the equatorial region and in the summer hemisphere. As in Holton (1983) the integration was carried out globally for an annually varying radiative drive. However, since topographic waves can reach the mesosphere only during the winter season, the results shown below depict only the winter hemisphere.

3. Results and discussion

The model was initialized to zonally symmetric conditions 60 days prior to the Northern Hemisphere winter solstice and integrated forward to the solstice, at which time the mean zonal wind and gravity wave induced mesospheric planetary wave were in quasi-steady balance. Various aspects of the resulting circulation are depicted in the figures. The mean zonal wind and zonally averaged wave drag distributions (Figs. 1 and 2) are nearly identical to the zonally symmetric model results shown in Figs. 2 and 4 of Holton (1983). In the present case, however, the strong zonal dependence of the gravity wave source produces a wavenumber 1 component of the wave

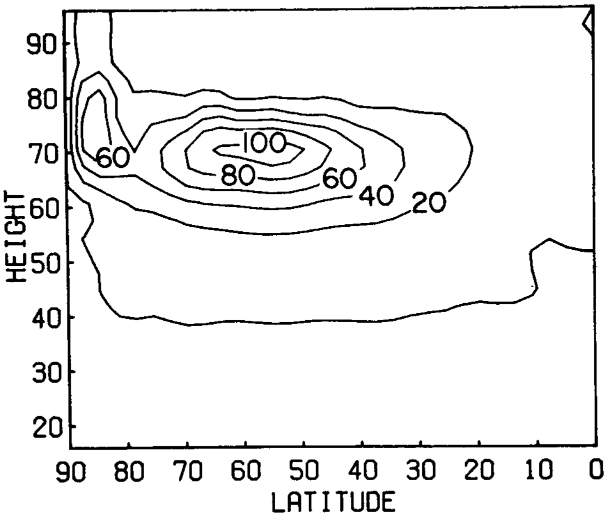

FIG. 3. Amplitude of planetary wavenumber 1 component of the wave drag force (m s^{-1} day^{-1}) at winter solstice (day 60).

drag force (Fig. 3) which is comparable in amplitude to the zonal mean drag force.

The latitude–height distribution of the geopotential amplitude of the planetary wave excited by the zonally asymmetric drag force is shown in Fig. 4. The perturbation is a maximum at the level of maximum forcing (=70 km) and decays away from that level both upward and downward. Although the EP fluxes (not shown) are directed upward and downward away from the 71 km level, their magnitudes are very small. In effect the wave is close to equivalent barotropic in structure and has very little interaction with the mean zonal flow.

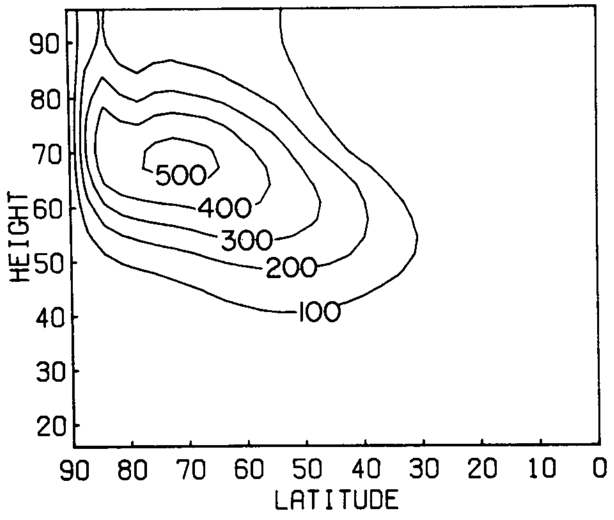

FIG. 4. Amplitude of the wavenumber 1 geopotential perturbation (m) excited by the wave drag shown in Fig. 3.

Despite the somewhat passive nature of the induced planetary wave in the present model, it does greatly alter the appearance of the mesospheric circulation near the 71 km level. In Fig. 5 the wave drag force and the zonal velocity at 71 km are plotted on a polar stereographic projection. Particularly noteworthy is the fact that the maximum wave drag does not

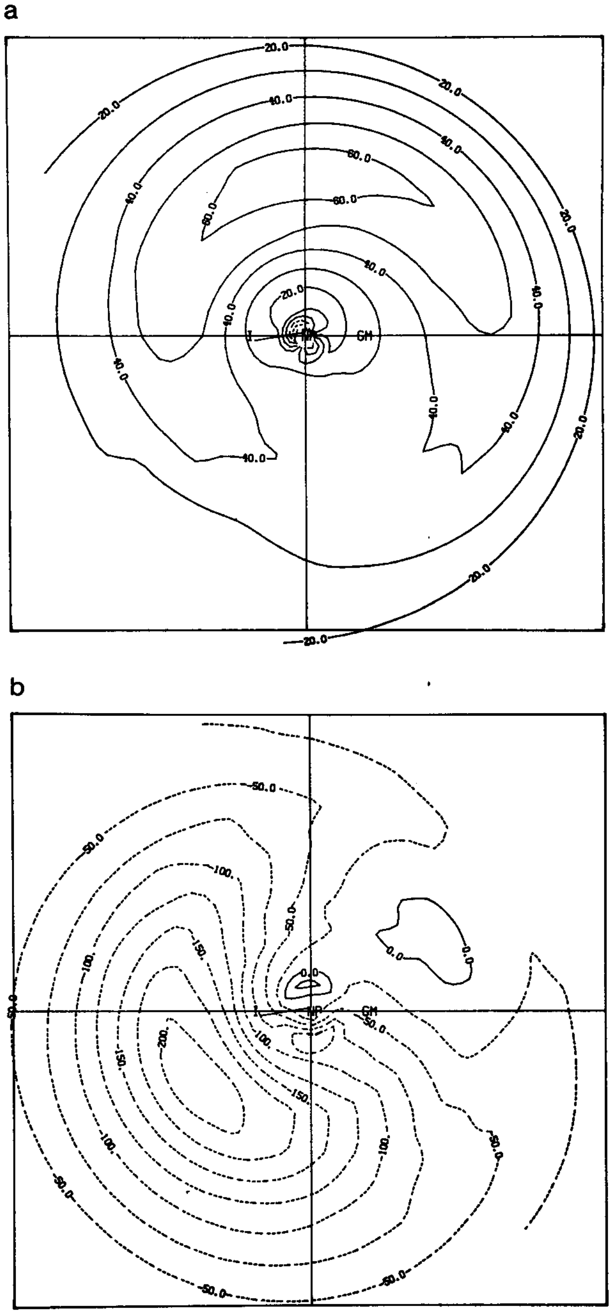

FIG. 5. Polar stereographic projections of the zonal wind speed (a) and the wavedrag force (b) at the 71 km level for Northern Hemisphere winter solstice. Wind speed in m s^{-1}; wave drag force in m s^{-1} day^{-1}.

coincide with the weakest zonal flow, but occurs 90 degrees downstream from the longitude of zonal wind maximum in the jet exit region. In this region the vorticity balance is analogous to the Sverdrup balance of the wind-driven ocean circulation. The curl of the wave drag force generates positive (negative) vorticity equatorward (poleward) of the jetstream axis. These tendencies are balanced by the planetary vorticity advection due to the diffluent meridional flow of the jet exit region, which causes positive (negative) planetary vorticity advection poleward (equatorward) of the jetstream axis.

The present results are of course based on a rather idealized model. Here we have used the Lindzen (1981) parameterization without consideration of modifications that may occur when gravity wave heat fluxes are included (e.g., Schoeberl *et al.*, 1983). However, this simplification seems justified in the present case since such effects are almost certainly secondary to the effect of the wave drag on the momentum budget, at least so far as the general circulation of the mesosphere is concerned. The present work provides some specific evidence that longitudinal variability in gravity wave sources may be a significant factor in determining the circulation of the middle atmosphere. Further progress along these lines must to some extent at least be dependent on the acquisition of an observed climatology of gravity wave sources.

Acknowledgments. This work was supported by the National Science Foundation's Atmospheric Research Section under NSF Grant ATM-8314111 and by the National Aeronautics and Space Administration, NASA Grant NAG2-66.

REFERENCES

Dunkerton, T. J., and N. Butchart, 1984: Propagation and selective transmission of internal gravity waves in a sudden warming. *J. Atmos. Sci.*, **41**, 1443–1460.

Fritts, D. C., 1984: Gravity wave saturation in the middle atmosphere: A review of theory and observations. *Rev. Geophys. Space Phys.*, 22, (in press).

Holton, J. R., 1983: The influence of gravity wave breaking on the general circulation of the middle atmosphere. *J. Atmos. Sci.*, **40**, 2497–2507.

——, and W. M. Wehrbein, 1980: The role of forced planetary waves in the annual cycle of the zonal mean circulation of the middle atmosphere. *J. Atmos. Sci.*, **38**, 1504–1509.

Lindzen, R. S., 1981: Turbulence and stress due to gravity wave and tidal breakdown. *J. Geophys. Res.*, **86P**, 9707–9714.

——, 1984: Gravity waves in the mesosphere. *Dynamics of the Middle Atmosphere*, J. R. Holton and T. Matsuno, Eds., Terra Scientific, 3–18.

Schoeberl, M. R., and D. F. Strobel, 1984: Nonzonal gravity wave breaking in the winter mesosphere, *Dynamics of the Middle Atmosphere*, J. R. Holton and T. Matsuno, Eds., Terra Scientific, 45–64.

——, —— and J. P. Apruzese, 1983: A numerical model of gravity wave breaking and stress in the mesosphere. *J. Geophys. Res.*, **88**, 5249–5259.